

# Accelerated Computation with Automatic Error Control of Light Water Thermodynamic Properties for LWR Safety Analysis

Luiz Felipe de Paula Carvalho, lfcarvalho@oceanica.ufrj.br

Eduardo Gomes Dutra do Carmo, egdcarmo@hotmail.com

Jian Su, sujian@con.ufrj.br

Nuclear Engineering Program, COPPE, Universidade Federal do Rio de Janeiro, Rio de Janeiro, Brazil

**Abstract.** *Rapid and accurate evaluation of thermodynamic properties as well as their derivatives is essential for the safety analysis of light water nuclear reactors (LWRs). In this work, we present a software package for accelerated calculation of light water thermodynamic properties and derivatives with automatic error control by using the discontinuous finite element method. The software package is based on the ASME Steam Table software that calculates thermodynamic properties of light water with high-degree polynomials. Although the ASME Steam Table provides industry standard water properties, it is not suitable for the safety analysis of light water nuclear reactors as real-time thermal-hydraulic simulation is required. Aiming at simulation in real time, the development of a software which has the same capacities of ASME Steam Table with the results being obtained in reduced time became necessary. Moreover, the derivatives of the thermodynamic properties can also be calculated by the present software, which however are not provided by the ASME Steam Table software. Numerical results showed that the calculation time of most thermodynamic properties has been much reduced compared with the ASME software while with automatically controlled errors.*

**Keywords:** *Thermodynamic properties, discontinuous finite element method, ASME Steam Table, light water reactor*

## 1. Introduction

The American Society of Mechanical Engineers (ASME) has feasible software, which calculates thermodynamic and transport properties, allowing the users to have properties with high order precision. Although this package provides industry standard water properties, it is not suitable for safety analysis when real-time simulation is required, because of the high order of the approximation polynomials that this package has. So that, an algorithm that propose a rapid way to calculate thermodynamics properties was developed. However, it is important to mention that there are other papers proposing what this paper proposes. Rodriguez et al. (2003) had proposed a similar algorithm, with the limitation that it only works to a previously specified thermodynamic phase. Pereira and Carmo (1997) have also proposed a method with the same goal, but it uses the continuous finite elements method, which also limits the algorithm. In this paper, we showed a method based on, due the computational performance and a great flexibility, the discontinuous finite elements (Discontinuous Galerkin Method, as is described in Carmo and Duarte, 2000, Duarte, Carmo and Rochinha, 2000 and Duarte, Rochinha and Carmo, 2000). It is used to generate steam tables to be used in a thermohydraulic simulator. An important feature of this method is that it uses ASME's software to calculate thermodynamics properties in a fewer time than this software, as is showed in this paper, and to get the derivatives of these properties, which are not provide by the ASME Steam Table software. For any specified domain, a structured and uniform grid is generated. To get more accurate values close to the curve, each element crossed by the water saturation curve will be treated like a new mesh, as will be showed in section 'Mesh Generation'. However, these meshes (called 'sub-meshes') will not be structured, because of some triangular and quadrangular sub-elements that will be defined by the saturation curve, as will be showed in section 'Sub-Elements Crossed by The Saturation Curve'. Then, we showed the procedure used to obtain, for a specific element, the coefficients of the polynomials that approach a hypothetic property, in section 'Mathematic Algorithm Description'. After that, in section 'Execution Time Algorithm Details', a rapid way to find the element that a point (T,P) is located is showed. Finally, some results comparing precision and elapsed time between ASME's package and the proposed method are analyzed.

## 2. Mesh Generation

It is known, from the thermodynamics, that in a saturation region, temperature ( $T$ ) can be expressed as a function of pressure ( $P$ ), and vice versa ( $T = f(P)$ ,  $P = f(T)$ ).

Looking to a 'Pressure x Temperature' diagram, a uniform bi-dimensional mesh will be generated, as well as a smaller bi-dimensional mesh inside each element that the saturation curve crosses (called 'sub-mesh', made to guarantee a better precision close to this curve), as figure 1 shows. To generate these meshes, some arguments will be used to specify the domain, such as: minimum and maximum temperatures of the domain ( $T_{min}$  and  $T_{max}$ , respectively); minimum and maximum pressures of the domain ( $P_{min}$  and  $P_{max}$ , respectively). The parameters that indicates the quality of the generated grid are: number of divisions in the  $T$  and  $P$  axis ( $NT$  and  $NP$ , respectively); and the number of subdivisions

in the  $T$  and  $P$  axis ( $NT_{sub}$  and  $NP_{sub}$ , respectively). These parameters are especially important in 'Execution Time Algorithm Details' section.

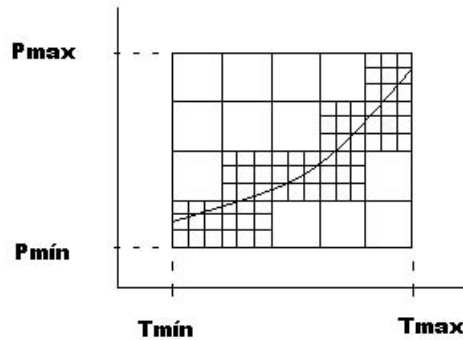


Figure 1. Mesh and Sub-mesh Generated to the specified domain

Once generated the meshes, the next step is to define, to each element and sub-element, the respective thermodynamic phase. The elements and sub-elements that the saturation curve does not cross are already to the calculation of the approximation polynomials. However, the sub-elements that are crossed by the saturation curve (there is no elements in this situation) will suffer a new sub-division, as shown in section 'Sub-Elements Crossed by The Saturation Curve'.

### 3. Sub-Elements Crossed by The Saturation Curve

It is possible to show that, in this case, the sub-elements will be always divided in two polygons, each with three, four or five sides, when the saturation curve inside the sub-element is approximated by a straight line. However, this paper will not work with five sides polygons. So, when a pentagon appears, it will be divided in two quadrilaterals, as showed by dotted straight line in Fig.2.

There are nine different situations that the saturation curve may cross a sub-element. Figure 2 shows these situations, with numbers indicating the sub-divisions that will be made.

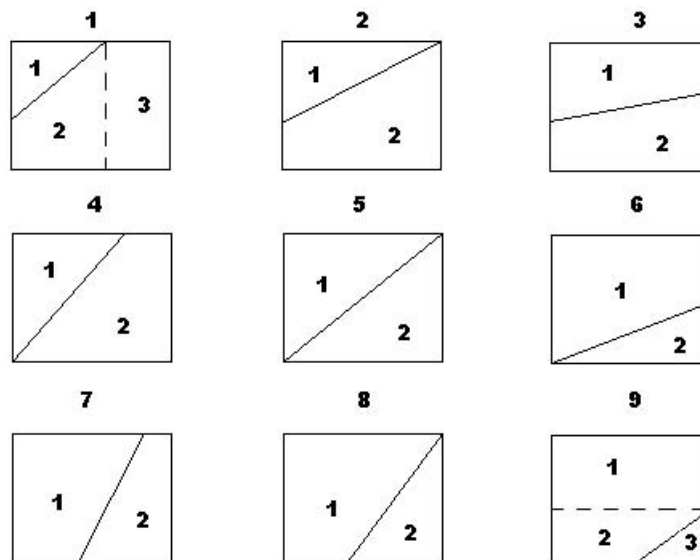


Figure 2. The nine different ways to the curve cross a sub-element

In each region of these sub-elements, approximation polynomials will be generated. Some details of how these polynomials are obtained are showed in 'Mathematic Algorithm Description' section.

#### 4. Mathematic Algorithm Description

To get the approximation polynomials, first of all, it is necessary to change the global coordinates into local coordinates (subsection 'Obtaining Local Coordinates'). Then, these coordinates are used to obtain coefficients of the approximation polynomials (subsections 'Obtaining the approximation polynomials to local coordinates' and 'Obtaining the approximation polynomials to global coordinates'). There are two different polynomials shown in this paper that approximate a hypothetical property. One of them based on local coordinates (shown in 'obtaining the approximation polynomials to local coordinates' subsection) and the other based on global coordinates (shown in 'obtaining the approximation polynomials to global coordinates' subsection). The second one uses the coefficients of the first one polynomial to calculate its own coefficients, and it has the advantage that a coordinates transformation is not necessary, so that properties can be calculated more quickly than the polynomials of the first method.

##### 4.1 Obtaining Local Coordinates

As in this paper, the elements will always be a rectangle, a quadrilateral or a triangle, a brief explanation about how the local coordinates  $(\xi_1, \xi_2)$  are obtained, is given.

- Rectangles (Fig.3) :  $\xi_1 = \frac{2(T-T_M)}{\Delta T}$  ,  $\xi_2 = \frac{2(P-P_M)}{\Delta P}$ , where  $T_M, P_M$  are the midpoint element coordinates, and  $\Delta T = \frac{(T_{max}-T_{min})}{NT}$  ,  $\Delta P = \frac{(P_{max}-P_{min})}{NP}$   
 Obs :  $-1.0 \leq \xi_1, \xi_2 \leq 1.0$

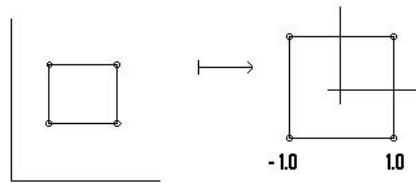


Figure 3. coordinates changing  $T - P \rightarrow \xi_1 - \xi_2$  to rectangles

- Triangles (Fig.4): consider  $L_1 = \frac{area_{BGC}}{area_{ABC}}$  ,  $L_2 = \frac{area_{AGC}}{area_{ABC}}$  e  $L_3 = \frac{area_{AGB}}{area_{ABC}} \Rightarrow L_1 + L_2 + L_3 = 1$ . The local coordinate given to an hypothetical point G will be  $G(L_1, L_2, L_3)$  (called area coordinates).

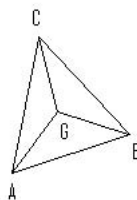


Figure 4. coordinates changing  $T - P \rightarrow L_1 - L_2 - L_3$  to triangles

Obs :  $0.0 \leq L_1, L_2, L_3 \leq 1.0$

- Quadrilaterals (Fig.5): consider an hypothetical quadrilateral element defined in  $T - P$ , the approximation  $F^h(T, P)$  written in terms of the local coordinates  $(\xi_1, \xi_2)$  is given by

$$F^h(\xi_1, \xi_2) = \sum_{i=1}^{NP_{integ}} x_i * \eta(\xi_1, i) * \eta(\xi_2, i) \quad (1)$$

And local coordinates

$$T(\xi_1, \xi_2) = \sum_{i=1}^{NP_{integ}} T(i) * \eta(\xi_1, i) * \eta(\xi_2, i) \quad (2)$$

$$P(\xi_1, \xi_2) = \sum_{i=1}^{NP_{integ}} P(i) * \eta(\xi_1, i) * \eta(\xi_2, i) \quad (3)$$

where  $(T(i), P(i))$  are the nodes coordinates of the element 'i'.

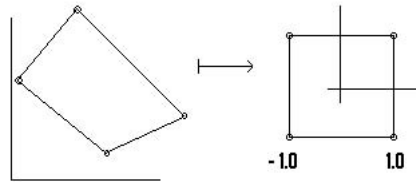


Figure 5. coordinates changing  $T - P \longrightarrow \xi_1 - \xi_2$  to quadrilaterals

Obs :  $-1.0 \leq \xi_1, \xi_2 \leq 1.0$

#### 4.2 Obtaining Approaches Polynomials to Local Coordinates

Consider  $F$  an hypothetic thermodynamic property ( $F(T, P) = F(T(\xi_1, \xi_2), P(\xi_1, \xi_2)) = F(\xi_1, \xi_2)$ ). The approximated function that will be obtained is :

$$F_1^h(T, P) = \sum_{i=1}^{npel} x(i, 1) * \eta(npel, i, \xi_1, \xi_2) \quad (4)$$

Where the coefficients  $x$  will be given by a linear-system solution  $A x = b_1$ , Where  $A$  and  $b$  are given by :

$$A_{i,j} = \int_{\Omega_e} \eta_i * \eta_j d\Omega = \sum_{l=1}^{NP_{integ}} w(l) * \det(l) * \eta_i(l) * \eta_j(l) \quad (5)$$

$$b_1(j) = \sum_{l=1}^{NP_{integ}} \eta_l * F(T(\xi_1, \xi_2), P(\xi_1, \xi_2)) \quad (6)$$

The same way to obtain the coefficients of the function  $F$  will be used in derivatives cases of  $F$ . The only necessary change that has to be made is the independent terms vector, which will be obtained by:

$$b_2(j) = \sum_{l=1}^{NP_{integ}} \eta_l * \frac{\partial F(T(\xi_1, \xi_2), P(\xi_1, \xi_2))}{\partial T} \quad (7)$$

$$b_3(j) = \sum_{l=1}^{NP_{integ}} \eta_l * \frac{\partial F(T(\xi_1, \xi_2), P(\xi_1, \xi_2))}{\partial P} \quad (8)$$

These linear-systems appears from quadratic residual errors, showed below:

$$J_1 = \int_{\Omega_e} [F_1^h - F]^2 d\Omega \quad (9)$$

$$J_2 = \int_{\Omega_e} \left[ F_2^h - \frac{\partial F}{\partial T} \right]^2 d\Omega \quad (10)$$

$$J_3 = \int_{\Omega_e} \left[ F_3^h - \frac{\partial F}{\partial P} \right]^2 d\Omega \quad (11)$$

Looking for the minimum errors, is imposed that:

$$\frac{\partial J_1}{\partial x(i, 1)} = 0 \quad (12)$$

$$\frac{\partial J_2}{\partial x(i, 2)} = 0 \quad (13)$$

$$\frac{\partial J_3}{\partial x(i, 3)} = 0 \quad (14)$$

From this derivatives, the previously mentioned linear-systems appear.

### 4.3 Obtaining Approaches Polynomials to Global Coordinates

Although the properties polynomials can be calculated as showed above, the function that we obtained depends on the local coordinates, and it spends a considerable time to be calculated. Looking for the fastest way to calculated the properties in execution time, it is interesting to have these properties as a direct function of the Temperature and Pressure ( $T, P$ ), and this method is showed in the explanations below.

#### 1. Quadrilaterals

Consider  $F(T, P)$  an hypothetic thermodynamic property, and  $x_1, x_2, x_3, x_4$  the coefficients of the local coordinate polynomial. The new coefficients  $C_1, C_2, C_3, C_4$  will be generated in such a way that we can approximate  $F(T, P)$  by the following function:

$$F(T, P) = C_1 + C_2T + C_3P + C_4TP \quad (15)$$

Once the four points of the quadrilateral are

$(T_1, P_1); (T_2, P_2); (T_3, P_3); (T_4, P_4)$ ,

five  $\mathbb{R}^4$  vectors can be made

$V_1 = (1; 1; 1; 1), V_2 = (T_1; T_2; T_3; T_4), V_3 = (P_1; P_2; P_3; P_4), V_4 = (T_1.P_1; T_2.P_2; T_3.P_3; T_4.P_4)$  and  $b = (x_1; x_2; x_3; x_4)$

The coefficients  $P_1, C_2, C_3, C_4$  will be the solution of the linear system  $\sum_{i=1}^4 M_{ij}.C_j = B_i$ , where

$$M_{11} = V_1 \bullet V_1, M_{12} = V_1 \bullet V_2, M_{13} = V_1 \bullet V_3, M_{14} = V_1 \bullet V_4,$$

$$M_{21} = M_{12}, M_{22} = V_2 \bullet V_2, M_{23} = V_2 \bullet V_3, M_{24} = V_2 \bullet V_4,$$

$$M_{31} = M_{13}, M_{32} = M_{23}, M_{33} = V_3 \bullet V_3, M_{34} = V_3 \bullet V_4,$$

$$M_{41} = M_{14}, M_{42} = M_{24}, M_{43} = M_{34}, M_{44} = V_4 \bullet V_4$$

and  $B_1 = b \bullet V_1, B_2 = b \bullet V_2, B_3 = b \bullet V_3, B_4 = b \bullet V_4$ , where ' $\bullet$ ' means scalar product.

#### 2. Triangles

Consider  $F(T, P)$  an hypothetic thermodynamic property, and  $x_1, x_2, x_3$  the coefficients of the local coordinate polynomial. The new coefficients  $C_1, C_2, C_3$  will be generated in such a way that we can approximate  $F(T, P)$  by the following function:

$$F(T, P) = C_1 + C_2T + C_3P \quad (16)$$

Once the three points of the triangle are

$(T_1, P_1); (T_2, P_2); (T_3, P_3)$ ,

four  $\mathfrak{R}^3$  vectors can be made

$V_1 = (1; 1; 1), V_2 = (T_1; T_2; T_3), V_3 = (P_1; P_2; P_3)$  and  $b = (x_1; x_2; x_3)$

The coefficients  $C_1, C_2, C_3$  will be the solution of the linear system  $\sum_{i=1}^3 M_{ij} \cdot C_j = B_i$ , where

$M_{11} = V_1 \bullet V_1, M_{12} = V_1 \bullet V_2, M_{13} = V_1 \bullet V_3,$

$M_{21} = M_{12}, M_{22} = V_2 \bullet V_2, M_{23} = V_2 \bullet V_3,$

$M_{31} = M_{13}, M_{32} = M_{23}, M_{33} = V_3 \bullet V_3,$

and  $B_1 = b \bullet V_1, B_2 = b \bullet V_2, B_3 = b \bullet V_3$ , where ' $\bullet$ ' means scalar product.

## 5. Execution Time and Algorithm Details

In execution time, a hypothetic point  $(T, P)$  localized in domain will be chosen by the user, and the thermodynamics properties, and the respective derivatives will be given. However, with the goal to have an efficient algorithm, is extremely necessary to find rapidly the element that the point is localized. Therefore, considering the elements numbered from down to up, and from the left to the right, the element where an hypothetic point  $(T, P)$  must be found is ' $ie$ ', which can be found by the following expression:

$$ie = NP * (j - 1) + i \quad (17)$$

where

$$i = \text{int}\left(\frac{T - T_{min}}{\Delta T}\right) + 1 \quad (18)$$

$$j = \text{int}\left(\frac{P - P_{min}}{\Delta P}\right) + 1 \quad (19)$$

$$\Delta T = \frac{T_{max} - T_{min}}{NT} \quad (20)$$

$$\Delta P = \frac{P_{max} - P_{min}}{NP} \quad (21)$$

where  $\text{int}$  is a function that returns the integer portion of a real number. It is important to emphasize that the parameters  $\Delta T$  and  $\Delta P$  are not calculated in execution time. In the case of the point is localized in a rectangular sub-element, similarly expressions will be utilized. If the point is localized in a sub-element which the saturation curve crosses, some simples verifying should be made, in order to find the region in the sub-element that the point is.

## 6. Results and Discussion

The analysis was made in a specific domain ( $T_{min} = 300$  F;  $T_{max} = 480$  F;  $P_{min} = 100$  psia;  $P_{max} = 500$  psia), considering two different properties, specific volume and viscosity.

Analysis of the medium error in the mesh as a whole, as well as an analysis looking to a specific point was made. To give an idea of the time spent by the ASME's software, and the efficiency of this algorithm, a comparison of the spent time by these two methods is also showed. It is important to say that in the proposed method, to spend less time as possible, the higher polynomial order is four (quadrilateral and rectangular cases).

### 6.1 Error Analysis to a Specific Point

In this analysis, the medium error and the elapsed time were analyzed for two chosen points, for specific volume and viscosity, as well as the corresponding derivatives. The two analyzed points was ( $T = 350$  F ;  $P = 350$  psia) and ( $T = 404$  F ;  $P = 247.5$  psia). The first point was chosen because it belongs to an element that the saturation curve does not cross. The second point was chosen because it is near from the saturation curve. The tables below shows these analysis.

Table 1. errors to ( $T = 350 F$  ;  $P = 350 psia$ )

Properties	Medium Error	elapsed time (ASME) (s)	elapsed time (Program) (s)	$\frac{elapsedtime(ASME)}{elapsedtime(Program)}$
$v$	$1.6424 \times 10^{-4}$	$0.4041 \times 10^{-6}$	$0.1017 \times 10^{-6}$	3.973
$\frac{\partial v}{\partial T}$	$9.7720 \times 10^{-4}$	$0.8833 \times 10^{-6}$	$0.1033 \times 10^{-6}$	8.551
$\frac{\partial v}{\partial P}$	$1.1299 \times 10^{-4}$	$0.7813 \times 10^{-6}$	$0.1567 \times 10^{-6}$	4.986
$\mu$	$8.3957 \times 10^{-4}$	$0.833 \times 10^{-6}$	$0.1021 \times 10^{-6}$	8.159
$\frac{\partial v}{\partial T}$	$1.6807 \times 10^{-3}$	$2.4467 \times 10^{-6}$	$0.1067 \times 10^{-6}$	22.931
$\frac{\partial v}{\partial P}$	$4.7860 \times 10^{-5}$	$2.5101 \times 10^{-6}$	$0.1567 \times 10^{-6}$	16.019

Table 2. errors to ( $T = 404 F$  ;  $P = 247,5 psia$ )

Properties	Medium Error	elapsed time (ASME) (s)	elapsed time (Program) (s)	$\frac{elapsedtime(ASME)}{elapsedtime(Program)}$
$v$	$2.9828 \times 10^{-3}$	$0.6431 \times 10^{-6}$	$0.1241 \times 10^{-6}$	3.973
$\frac{\partial v}{\partial T}$	$2.3594 \times 10^{-3}$	$0.8742 \times 10^{-6}$	$0.1561 \times 10^{-6}$	5.600
$\frac{\partial v}{\partial P}$	$5.7344 \times 10^{-3}$	$0.6243 \times 10^{-6}$	$0.1565 \times 10^{-6}$	3.989
$\mu$	$2.9692 \times 10^{-4}$	$0.8763 \times 10^{-6}$	$0.1271 \times 10^{-6}$	6.895
$\frac{\partial v}{\partial T}$	$2.8192 \times 10^{-4}$	$2.5302 \times 10^{-6}$	$0.1563 \times 10^{-6}$	16.188
$\frac{\partial v}{\partial P}$	$1.3769 \times 10^{-3}$	$2.2501 \times 10^{-6}$	$0.1264 \times 10^{-6}$	17.801

## 6.2 Error Analysis to the Domain as a Whole

In this analysis, the medium error and the elapsed time were analyzed in a domain as a whole, for specific volume and viscosity, as well as the corresponding derivatives. The number of points analyzed was 10000, and it was one point in each element of the mesh.

Table 3. errors to the domain

Properties	Medium Error	elapsed time (ASME) (s)	elapsed time (Program) (s)	$\frac{elapsedtime(ASME)}{elapsedtime(Program)}$
$v$	$2.6078 \times 10^{-5}$	$0.6305 \times 10^{-6}$	$0.1628 \times 10^{-6}$	3.9375
$\frac{\partial v}{\partial T}$	$6.3434 \times 10^{-5}$	$0.9325 \times 10^{-6}$	$0.1613 \times 10^{-6}$	5.8123
$\frac{\partial v}{\partial P}$	$7.7239 \times 10^{-5}$	$0.9416 \times 10^{-6}$	$0.3106 \times 10^{-6}$	3.0316
$\mu$	$6.1289 \times 10^{-6}$	$1.4103 \times 10^{-6}$	$0.3204 \times 10^{-6}$	4.4063
$\frac{\partial v}{\partial T}$	$2.1386 \times 10^{-5}$	$2.6632 \times 10^{-6}$	$0.3120 \times 10^{-6}$	8.536
$\frac{\partial v}{\partial P}$	$1.9206 \times 10^{-5}$	$2.6612 \times 10^{-6}$	$0.3113 \times 10^{-6}$	8.549

## 7. Conclusions

The proposed algorithm is shown to be efficient in calculating thermodynamic properties and their respective derivatives. While the calculated results are within acceptable accuracy compared with the ASME's values (values industrially accepted), the time spent in calculation are significantly less than the ASME's software. The present method can be used in safety analysis of light water nuclear reactors (LWRs). The precision can be as higher as the user specifies, and it is always significantly faster than ASME's software. More analysis will be made in specific situations that can generate problems with the errors when the elements magnitude are very different than the sub-elements magnitude.

## 8. REFERENCES

- ASME, Asme Steam Tables - sixth edition, New York, 1993
- O. C. Zienkiewicz, K. Morgan, Finite Elements and Approximation, Dover publications, New York, 1983.
- S. J. Chapman, Fortran 90/95 for Scientists and Engineers, McGraw-Hill.
- E. G. D. Carmo, A. V. C. Duarte, A Discontinuous Finite Element Based Domain Decomposition Method. Computer Methods in Applied Mechanics and Engineering, 190, pp. 825-843, 2000.
- A. V. C. Duarte, E. G. D. Carmo, F. A. Rochinha, Consistent Discontinuous Finite Elements in Elastodynamics, Computer Methods in Applied Mechanics and Engineering, 190 pp. 193-223, 2000.
- A. V. C. Duarte, F. A. Rochinha, E. G. D. Carmo, Discontinuous Finite Elements Formulations Applied to Cracked Elastic Domains, Computer Methods in Applied Mechanics and Engineering, 185, pp. 21-36, 2000.

- S. C. Brenner and L. R. Scott, *The Mathematical Theory of Finite Element Methods*, Springer-Verlag.
- L. C. M. Pereira, E. G. D. Carmo, *Geração de Aproximações para Correlações em Códigos de Análise Termo-Hidráulica*, Proceedings of 11th Meeting (XI ENFIR), Poço de Caldas, Brazil, August, 1997
- M. M. Rodrigues, D. R. Cerqueira, E. G. D. Carmo, J. Su, *Optimização Computacional da Tabela de Vapor ASME para a Simulação Termo-Hidráulica de Centrais Nucleares*, Anais do I Jornada de Iniciação Científica de Engenharia Química, UFRRJ, 2004.

## **9. Responsibility notice**

The authors are the only responsible for the printed material included in this paper.